Landscape Ecol (2010) 25:1575–1587
DOI 10.1007/s10980-010-9528-4

RESEARCH ARTICLE

Measuring boundary convexity at multiple spatial scales using a linear "moving window" analysis: an application to coastal river otter habitat selection

Shannon E. Albeke · Nathan P. Nibbelink · Lan Mu · Daniel J. Ellsworth

Received: 15 October 2009 / Accepted: 28 August 2010 / Published online: 19 September 2010

Abstract Landscape metrics have been used to quantify ecological patterns and to evaluate relationships between animal presence/abundance and habitat at multiple spatial scales. However, many ecological flows occur in linear systems such as streams, or across patch/landscape boundaries (ecotones). Some organisms and flows may depend on the boundary shape, but metrics for defining linear boundary characteristics are scarce. While sinuosity and fractal dimension address some elements of shape, they fail to specify the dominate shape direction (convexity/concavity). We propose a method for measuring boundary convexity and assess its utility, along with sinuosity and fractal dimension, for predicting site selection by coastal river otters. First, we evaluate the characteristics of boundary convexity using a hypothetical boundary. Second, to compare convexity with other linear metrics boundary convexity, sinuosity and fractal dimension were calculated for the coastline of a set of islands in Prince William Sound, AK. Finally, we use logistic regression in an information-theoretic framework to assess site selection of river otters as a function of these linear metrics. Boundary convexity, fractal dimension and sinuosity are relatively uncorrelated at all scales. Otter latrine sites occurred at significantly more convex locations on the coastline than random sites. Using logistic regression and convexity values at the 100 m window-size, 69.5% of the latrine sites were correctly classified. Coastal terrestrial convexity appears to be a promising landscape-scale metric for predicting otter latrine sites. We suggest that boundary convexity may be an important landscape metric for describing species use or ecological flows at ecotones.

Keywords Ecotone · Sinuosity · Fractal dimension · Boundary shape · *Lontra canadensis* · Landscape and patch metrics

S. E. Albeke (✉) · N. P. Nibbelink
Warnell School of Forestry and Natural Resources, University of Georgia, Athens, GA 30602, USA

Present Address:
S. E. Albeke
Wyoming Geographic Information Science Center, University of Wyoming, Dept. 4008, 1000 E. University Ave., Laramie, WY 82071, USA
e-mail: salbeke@uwyo.edu

L. Mu
Department of Geography, University of Georgia, Athens, GA 30602, USA

D. J. Ellsworth
College of Natural Sciences, University of Texas Austin, Austin, TX 78712, USA

Introduction

The use of landscape and patch metrics to measure broad-scale ecological patterns has become increasingly more common (Turner 1989; Wu 2004; Kearns et al. 2005; Hopkins 2009), in particular for

describing relationships between animals and their habitat (Hamer et al. 2006; Forester et al. 2007; Grober-Dunsmore et al. 2008). Patch shape is often identified as important for determining species presence (Heegaard et al. 2007; Taylor et al. 2008), animal density (Ewers and Didham 2007), the distribution of organisms within a patch (Haynes and Cronin 2006) and has been shown to influence the movement of nutrients (Polis and Hurd 1996). Patch shape is most often measured as the perimeter-to-area ratio or patch fractal dimension (McGarigal et al. 2002; Rempel 2008). However, some ecological relationships may depend more heavily on characteristics of patch boundaries than on whole patch properties (such as animal–habitat relationships when "edge" habitat characteristics are important to the species). To measure characteristics of boundaries we have largely been limited to the conventional whole patch metrics, or relatively simple measures on boundary segments themselves, such as sinuosity. In order to improve our understanding of how boundary shape may influence ecological processes or animal habitat selection, we need more refined metrics for defining boundary shape. One such metric is boundary convexity. The degree of convexity (or concavity) for a defined boundary may be important to organisms or flow under a variety conditions much in the same way that topographic concavity (valleys) or convexity (ridges) are important to habitat use by elk (Kie et al. 2005) or movement of soil particles (Ruiz et al. 2006). However, in an extensive literature search, we have not found an ecological study that has substantially dealt with convexity of an ecotone, edge, or boundary as important to ecological processes or organism–environment relationships. Here we offer an approach for calculating boundary convexity at multiple spatial scales (script available free online; Albeke et al. 2009), then we demonstrate the value of boundary convexity for describing habitat selection for coastal river otters.

Any understanding of animal habitat selection necessitates consideration of spatial scale. Each organism's perspective dictates the scale at which it observes the physical world (Allen and Hoekstra 1992). The scale, shape and juxtaposition of landscape patches can affect species abundance and distribution. For example, McGrath et al. (2003) found a reduced ability to discriminate northern goshawk (*Accipiter gentilis*) nest sites from available habitat as landscape scale increased while Mitchell et al. (2001) found that coarser landscape characteristics are most important for prediction of migratory bird species breeding habitat. Additionally, Nams et al. (2006) found that variables most important for predicting grizzly bear (*Ursus arctos*) habitat selection varied depending on the spatial scale at which the variables were averaged. Thus, investigating the influence of scale in determining (and measuring) how organisms respond to their environment has been, and still is, a critical area of research. This work can help tackle scale-related issues of geospatial data analysis in general, and avoid scale traps such as ecological fallacy (Robinson 1950) and aggregation effects (King et al. 2004).

Fractals can be used to represent many kinds of patterns and all spatial scales can be represented through self-similarity (Li 2000). The fractal dimension can be calculated for any portion of a patch's boundary for any scale. This value can be used to quantify the complexity of the feature at the given scale. Unfortunately, the fractal dimension will not describe the direction of a complex feature relative to the adjacent features. Our research required a method to quantify the shape of a portion of a patch's boundary relative to its adjacent features. We have developed an approach for calculating boundary convexity, a new landscape metric that quantifies the shape of a patch boundary (ecotones, edges or other linear features). We define boundary shape as either convex or concave. Convexity is considered a pattern metric in landscape ecology (Trani and Giles 1999). The degree of convexity can be unique for any point along the patch (or landscape) boundary and will vary with spatial scale. Because of this trait, convexity may provide a biologically meaningful measurement describing the use of boundaries by wildlife.

Coastal river otters forage for fish within the intertidal zone of islands located in Prince William Sound, Alaska and choose specific locations for their latrines along the coastline (Ben-David et al. 1998, 2005; Bowyer et al. 2003). This results in the transport of nutrients from the marine environment to the coastal terrestrial community (Ben-David et al. 1998) which has a significant influence on the vegetation community, both through nutrient enrichment and disturbance by river otters (Roe et al. 2010). Otter latrines are used as communication tools, with

social otters advertising group associations and dominance while solitary otters use latrines to facilitate mutual avoidance (Rostain et al. 2004; Ben-David et al. 2005). Ben-David et al. (2005) hypothesized that the combination of large intertidal rock (scent marking platforms) and the presence of old-growth forest (prevention of scent-mark dehydration) provide the greatest influence on otter latrine site selection. Because appropriate scent-marking platforms are often on points (Larsen 1983), and the fact that scent dispersal may be facilitated by wind, we hypothesize that coastal shape will be a significant driver of latrine site selection. In particular, we hypothesize that otters are more likely to choose latrine sites whose coastline is sinuous (has more points and bays) at broader scales (500–1,000 m), and more convex at local scales (10–200 m). The objectives of our study are threefold: (1) to characterize boundary convexity using a hypothetical boundary of known dimensions; (2) to calculate boundary convexity of a coastline in Prince William Sound, Alaska, and compare its characteristics to sinuosity and fractal dimension; and (3) determine the spatial scale and linear metric most appropriate for describing coastal river otter latrine site selection.

Methods

Process for quantifying boundary convexity

The boundary convexity measure we propose can be used to quantify the relative convexity/concavity for any measure-point along a linear feature (e.g. patch boundary). Using route-events in ArcGIS™ (ESRI 2006) to represent the linear boundary feature, the spatial location of a given measure-point along the feature can be stored. The calculation of convexity becomes easier if the boundary is simplified. To simplify the boundary, a three-point circular arc representing the boundary segment is created. The circular arc uses, in sequential order, the start-point (measure-point − (½ * window-size)), measure-point, and end-point (measure-point + (½ * window-size)) measures of the boundary segment (Fig. 1). The circular arc represents the relative shape of the boundary at the measure-point. The orientation (clockwise or counterclockwise) of the circular arc, in relation to the boundary segment, determines whether the patch portion is concave or convex (i.e. clockwise = convex). The degree of convexity is determined by obtaining the mid-point of the circular arc, mid-point of the chord connecting the start and end points, and finding the chord height between the mid-points (Fig. 1, Step 5). The value quantifying convexity is then a combination of the circular arc orientation (sign is positive for convex and negative for concave) and the chord height value described above. Boundary convexity can range from 0 to ± ½ the window-size (scale), with 0 indicating a straight boundary (on average) at the given scale, a positive value indicating a convex boundary, and a negative value indicating a concave boundary. Because the convexity value is calculated in map units (e.g. meters) it may be valuable for defining the relative size of landscape boundary features. However, because scale-independence is a valuable feature of a landscape metric we calculate the boundary convexity index (BCI) as:

$$\mathrm{BCI} = \mathrm{BC}/\mathrm{BC}_{\max} \quad (1)$$

where BC is the unscaled convexity value in meters and $\mathrm{BC}_{\max}$ is equal to ½ the scale (window-size). The BCI values are scale-independent and range between −1.0 and +1.0. Figure 2 demonstrates how BCI values can vary using an example patch boundary.

With the information gathered to calculate convexity, one can also calculate sinuosity (S):

$$\mathrm{S} = \mathrm{TL}/\mathrm{EL} \quad (2)$$

where TL is the total segment length (i.e. window-size) and EL the Euclidean distance between start and end points. Sinuosity values can range between 1 (straight line) and the total segment length and is scale-independent. The Boundary Convexity Tool (BCT, Albeke et al. 2009) can be used to calculate both sinuosity and convexity at multiple window-sizes (scales) and steps (positions along the feature).

The purpose for using route-events is twofold. First, routed layers allow for easily managed references to any location along the linear feature of interest via route measures. The route measures, in turn, allow for easy interpretation of the location (a measure is simply the distance in meters from the start of the line), easy manipulation (simple math to move a specified distance along the route) and simple and accessible storage of output (event tables).

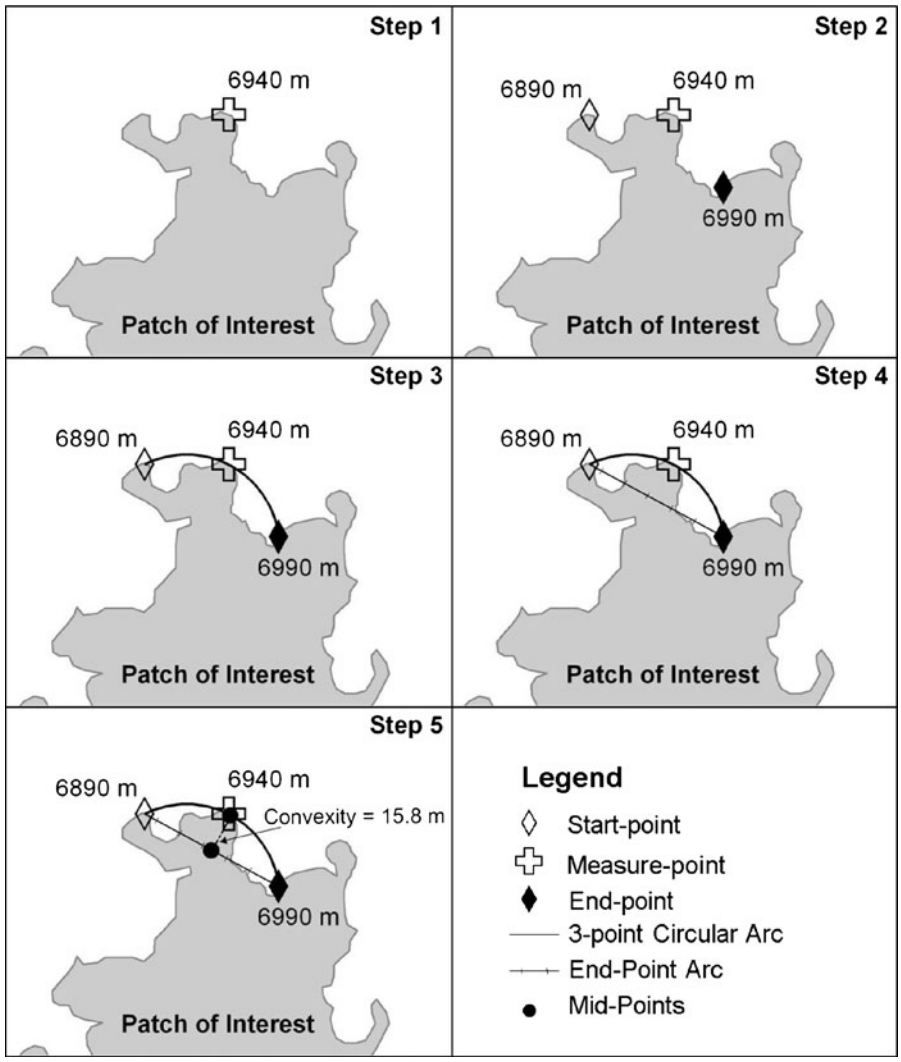

Fig. 1 The procedure to calculate boundary convexity: (1) obtain start, measure and end points (0, 50 and 100% of the length) of the boundary segment (Steps 1 and 2); (2) draw circular arc through the three points (Step 3); (3) determine circular arc orientation (clockwise or counterclockwise); (4) draw a chord between start and end points (Step 4); (5) obtain the mid-point of the circular arc and chord (Step 5); (6) calculate the chord height. For this particular example, the boundary convexity value is equal to 15.8 m, indicating the measure-point is convex given a window-size of 100 m

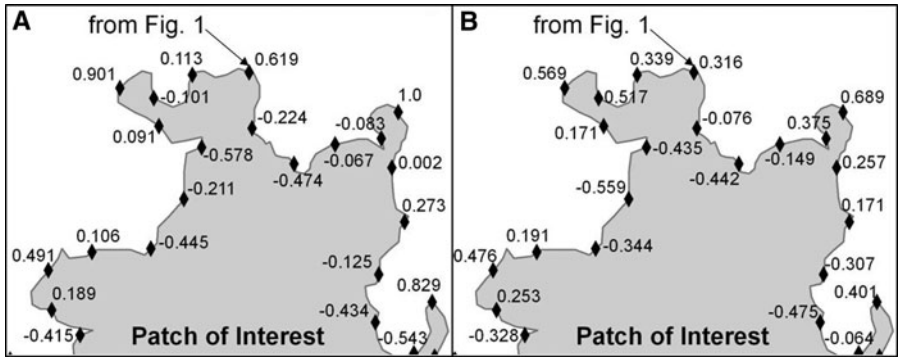

Fig. 2 An example of boundary convexity index (BCI) values for a window-size of 50 m (**a**) and 100 m (**b**) and a step-size of 20 m. Positive values indicate convexity while negative values indicate concavity. Please note the BCI value differences between the same measure-points at the two scales (window-sizes)

Construction of known dimension dataset

We constructed a 'saw-toothed' shaped line to mimic a portion of a hypothetical patch boundary with known dimensions to illustrate the range of convexity values given a range of boundary shape conditions. In the horizontal direction, the peaks and troughs of the hypothetical patch boundary (Figs. 3, 4) are 200 m

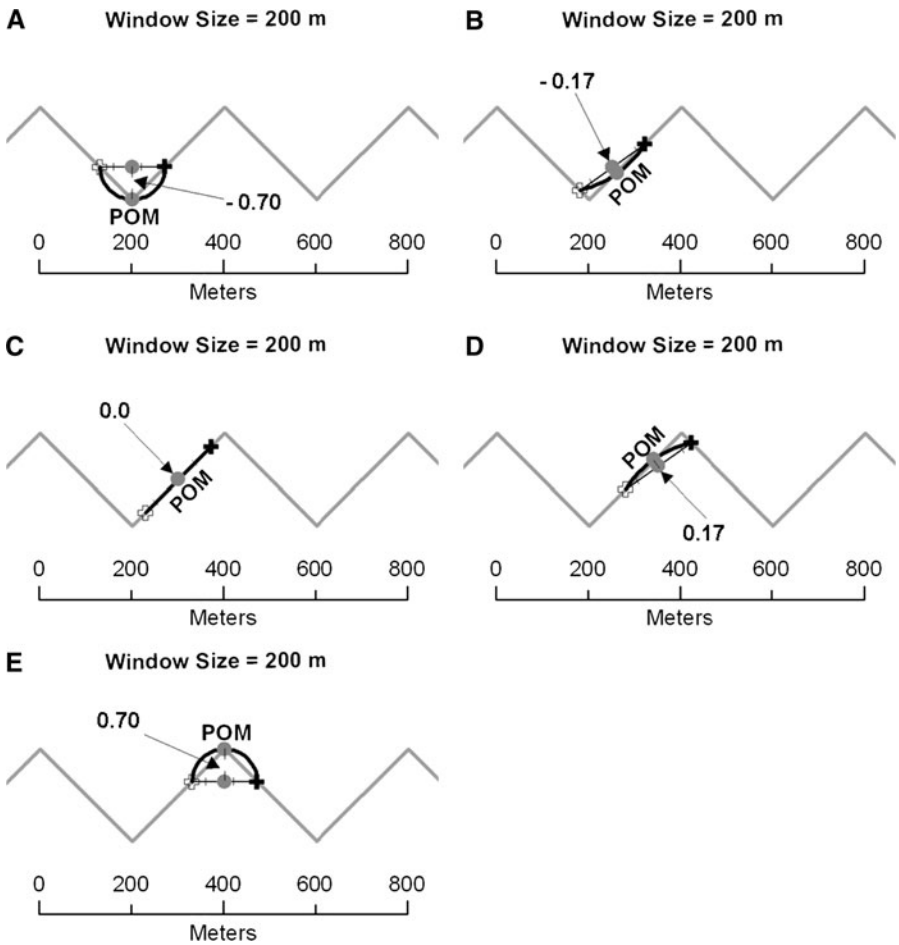

Fig. 3 An example of how boundary convexity index values change as the measure-point (POM) changes using a window-size of 200 m. The measure-point begins at a trough of the wave (**a**), 25% of the segment distance (**b**), 50% of the segment distance (**c**), 75% of the segment distance (**d**), and ends at a peak of the wave (**e**)

apart and the line segment connecting these extreme locations is 282.8 m in length. First, to demonstrate how different locations along a patch's boundary can affect boundary convexity, five separate locations on the patch boundary and a window-size of 200 m was used. The chosen measurement points were located at 0% (trough), 25, 50, 75 and 100% (peak), of a patch boundary line. Second, to demonstrate how changes in scale affect boundary convexity, four different window-sizes were applied to a constant location (at a peak) of the hypothetical patch boundary. The chosen window-sizes were 200, 500, 1000 and 1132 m (Fig. 4a–d). The saw-toothed design was used (as opposed to a more "natural" shape) due to the simplicity for creation, visualization and interpretation. Results of analyzing a more curvilinear feature would have been similar; however the arcs demonstrating the calculation would have been more difficult to see.

Comparing boundary metrics

In order to characterize the behavior of the boundary convexity metric across a range of natural conditions, we compared BCI values to two other metrics commonly used for linear features, sinuosity and fractal dimension. In addition, because statistical analysis of species–environment relationships often depends on independent predictor variables, we wanted to determine whether boundary convexity was a unique metric. Our test area was a coastline (marine-terrestrial boundary) located in southwestern Prince William Sound, Alaska. Coastlines in the Knight Island complex (including Disk, Eleanor and Ingot Islands; 147°43′ W, 60°30′ N) were digitized using IKONOS 1-m panchromatic images, at a scale of 1:1,500, creating a coastline 245 km in length. The island polygons were then converted into a route feature class, which is required for the BCT (Albeke

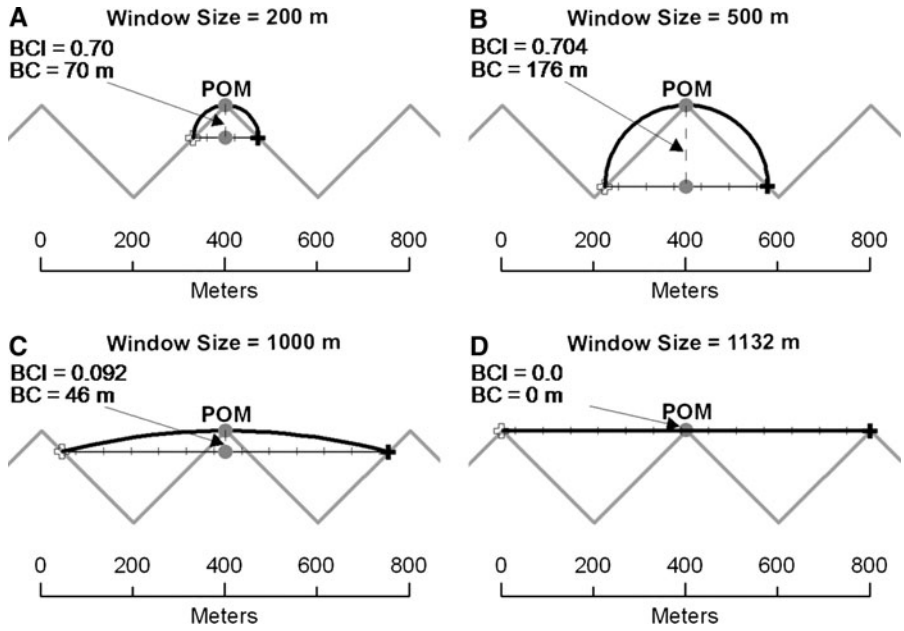

Fig. 4 An example of how boundary convexity (BC) in meters and boundary convexity index (BCI) values change as window-size (scale) increases for the same measure-point (POM). The window-sizes are 200 m (**a**), 500 m (**b**), 1,000 m (**c**), and 1,132 m (**d**)

et al. 2009). BCI (Eq. 1) and sinuosity (Eq. 2) were calculated for the entire coastline at seven window-sizes, 10, 20, 50, 100, 200, 500 and 1,000 m and a step-size (moving-window increment) of 10 m using the BCT. Fractal dimension was also calculated for each window-size. To calculate fractal dimension, each coastline segment spatial extent was found and the maximum difference between the X coordinates and the Y coordinates was stored. Next, five separate ruler sizes were created by taking 1, 5, 10, 20 and 40% of the maximum coordinate difference. The rulers are then placed end-to-end along the boundary segment to give a total segment length given the ruler size. The fractal dimension was calculated using the log–log relationship:

$$\mathrm{Log}(\mathrm{L}(\mathrm{s})) = (1 - \mathrm{D})\mathrm{Log}(\mathrm{s}) + \mathrm{b} \quad (3)$$

where L is the length of the ruler (s) multiplied by the number of rulers needed to measure the total boundary segment, $1 - \mathrm{D}$ is the slope and D is the fractal dimension (Mandelbrot 1982). Fractal dimension values are scale-independent and can range between 1 (straight line) and 2 (highly complex line) (Mandelbrot 1982; Turchin 1996).

For each window-size (scale), BCI, the absolute (or directionless) BCI, sinuosity and fractal dimension were compared using Pearson's r correlation coefficient to assess similarity between the metrics. All statistical analyses were performed using SAS 9.1 (SAS Institute Inc., Cary, NC).

Application to coastal river otters

During the summer of 2006, 326 river otter latrine sites were identified along the coastline and GPS locations were recorded. GPS locations were snapped to the island boundaries (coastline route features) with Knight Island having 257, Disk Island 23, Eleanor Island 38, and Ingot Island 8 latrine locations, respectfully. To determine whether linear metrics, including convexity index, sinuosity and fractal dimension, influence otter latrine site selection, 326 random locations were identified. Random locations were a minimum of 100 m from an existing latrine or other random location.

Logistic regression with an information-theoretic approach was used to determine which boundary metric (across a range of spatial scales) best fit the data. Twenty-eight candidate models, each consisting of a single variable; BCI, absolute BCI, sinuosity and fractal dimension at each of the spatial scales (10, 20, 50, 100, 200, 500, 1000 m), were compared. Methods followed the approach of Anderson et al. (2000). To test for goodness-of-fit (GOF), the Hosmer–Lemeshow

GOF statistic was calculated for the global model (Hosmer and Lemeshow 2000). The global model consisted of the entire set of available variables.

Akaike's Information Criteria (AIC) uses maximum likelihood to estimate the relative model fit (Burnham and Anderson 2001). However, this approach may create biased results for small samples size. Burnham and Anderson (2001) suggest correcting for small sample size:

$$\mathrm{AIC_c} = -2\ln(\mathrm{L}(\widehat{\theta} \mid \mathrm{data})) + 2\mathrm{K} + (2\mathrm{K}(\mathrm{K}+1)/(\mathrm{n}-\mathrm{K}-1)) \quad (4)$$

where $\ln(\mathrm{L}(\widehat{\theta} \mid \mathrm{data}))$ is the maximized log-likelihood over the unknown model parameters (θ) given the data, and K is the number of parameters in the approximating model. As sample size (n) increases, $\mathrm{AIC_c}$ approaches the same AIC value. Models with lower $\mathrm{AIC_c}$ values are deemed to be better representations of the process being modeled. Akaike weights were calculated to determine the weight of evidence (w_i) for each model within the candidate set:

$$w_i = \frac{\exp(-\Delta\mathrm{AIC_{c_i}}/2)}{\sum_{r=1}^{R}\exp(-\Delta\mathrm{AIC_{c_r}}/2)} \quad (5)$$

where $\Delta\mathrm{AIC_{c_i}}$ is the $\Delta\mathrm{AIC_{c_r}}$ value for the *i*th model in the set of R candidate models (Burnham and Anderson 2001). The value of w_i can range from 0 to 1. The candidate model with the largest w_i can be said to be the best approximating model.

Two methods were used to assess relative precision of the logistic models. First, a leave-one-out cross-validation technique was used to determine the expected model error rate (Steyerberg et al. 2001). To perform leave-one-out cross-validation, each sample record is left out, while the rest of the records are used to generate a model. This model is then used to predict presence or absence of the latrine for the left out record. The process is repeated so that each record is excluded from model fitting once, allowing for prediction and classification error rates to be determined. Model predictions ≥ 0.5 indicated latrine presence and predictions <0.5 indicated latrine absence. Secondly, Receiver Operating Characteristic (ROC) plots were generated and area under the curve (AUC) was calculated.

Results

Changes in convexity with location

Boundary convexity index (BCI) values range from -1 (concave) to $+1$ (convex), the magnitude of which depends both on the position of the measure-point on the boundary (Fig. 3) and on the window-size (Fig. 4). As the measure-point moves from the trough to the peak (with window-size = 200 m and 4 equal steps), the BCI value ranges from -0.70 to -0.17, 0.0, 0.17, and finally 0.70 (Fig. 3a–e). In the hypothetical boundary, because of the regular geometry, the value of concavity at the trough is equal to and opposite the convexity at the peak. In reality, the maximum convexity will be driven in part by the maximum distance from peak to trough (points to bays in case of a coastal boundary), and in part by the window-size.

Changes in convexity with scale

As window-size (scale) increases from 200 to 500 m, unscaled boundary convexity increases because the 200 m window-size is substantially shorter than the trough to trough distance of the hypothetical boundary, whereas the 500 m window-size approaches the trough to trough distance (Fig. 4a, b). However, because BCI is scale independent, the values are nearly identical. In this example, the maximum unscaled boundary convexity value would be measured when the measure-point is at a peak and the window-size is equal to the wavelength, 566 m, whereas BCI would remain relatively unchanged. As window-sizes increase in scale beyond the wavelength, the convexity values decrease until reaching a value of 0 when the window-size (1,132 m) encompasses the two adjacent peaks to the measure-point (Fig. 4c, d). A value of zero will occur whenever the conditions of the boundary conspire to create a straight line between the endpoints and the measure-point, regardless of intervening boundary complexity.

Comparison of patch boundary metrics

Comparisons between BCI, absolute BCI, fractal dimension and sinuosity indicate that these linear metrics are relatively uncorrelated for our study area

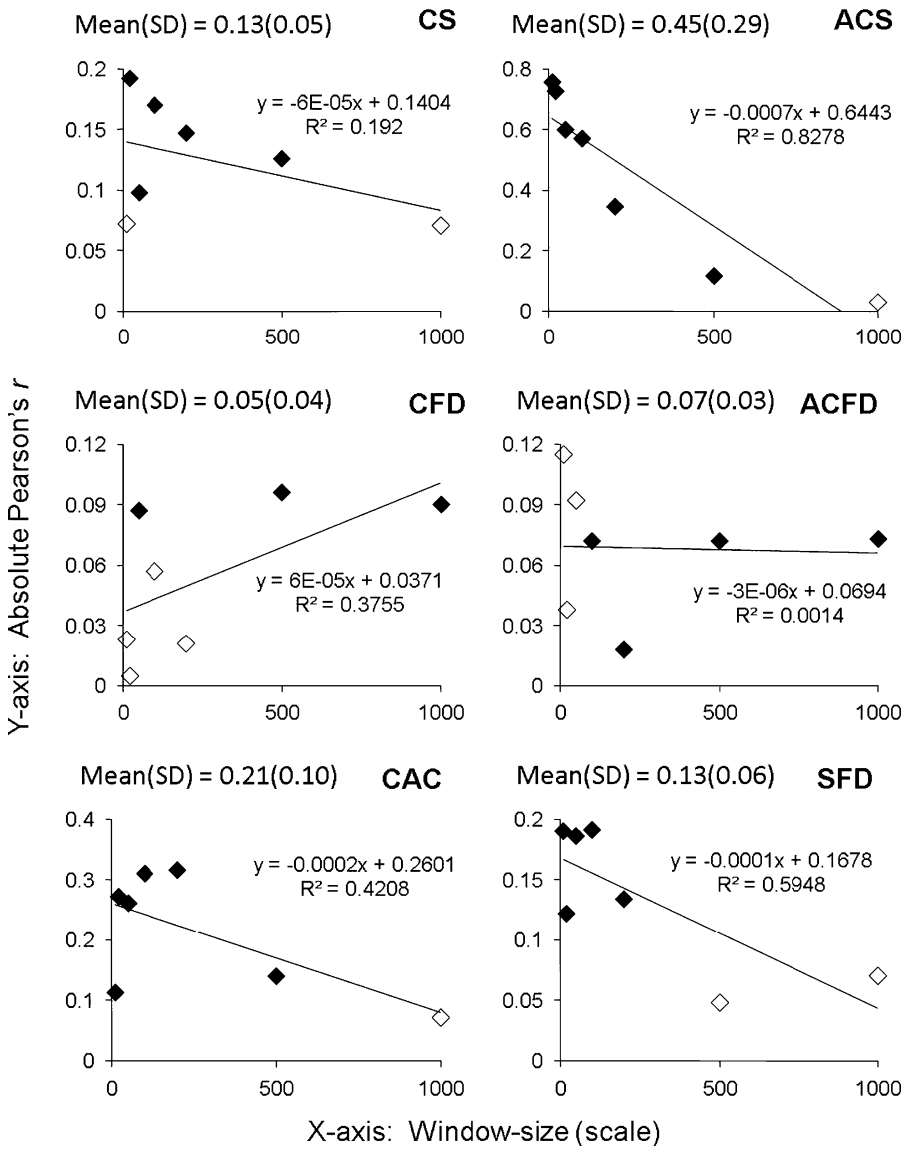

Fig. 5 Scatter plots of absolute Pearson's *r* correlation coefficients across all window-sizes for each patch boundary metric combination (*CS* convexity-sinuosity, *ACS* absolute convexity-sinuosity, *CFD* convexity-fractal dimension, *ACFD* absolute convexity-fractal dimension, *CAC* convexity-absolute convexity, *SFD* sinuosity-fractal dimension). *Solid symbols* indicate significance at the 95% confidence level ($P < 0.05$) and *hollow symbols* are not significant. Mean (SD) Pearson's *r* across all window-sizes, trend lines, the associated linear equations and R^2 values are included

at all scales (Fig. 5). The mean absolute Pearson's *r* was greatest between absolute BCI and sinuosity ($\mu = 0.45$) and smallest between BCI and fractal dimension ($\mu = 0.05$; Fig. 5). One exception is absolute BCI and sinuosity, which are correlated for window-sizes < 200 m (Pearson's $r > 0.5$, Fig. 5). This was not unexpected given that both sinuosity and absolute BCI measure aspects of line complexity (how much it "meanders" between two points) and ignore shape direction. However, at larger scales, the relationship between absolute BCI and sinuosity weakens, seemingly because sinuosity values increase in range at larger scales (Table 1). We must note here that the sinuosity calculation can produce outlying values (erroneously high) when the two end points are very close, but the scale (window-size) is very large, as in the case of islands. We excluded these outliers (<1% of our data) from our analysis.

The correlation coefficient varied with window-size (scale). For BCI versus sinuosity, absolute BCI versus sinuosity, BCI versus absolute BCI and sinuosity versus fractal dimension, the correlation coefficient decreased as window-size increased (Fig. 5). Conversely, as scale increased, the correlation between BCI and fractal dimension also increased.

Table 1 The mean (SD) and minimum, maximum values for each linear metric at each window-size (scale)

Window-size (m)	Boundary convexity index	Sinuosity	Fractal dimension
10	0.032 (0.265)	1.12 (0.19)	1.06 (1.32)
	−0.804, 0.827	1.00, 3.26	1.00, 1.16
20	0.083 (0.306)	1.24 (0.37)	1.07 (0.03)
	−0.906, 1.0	1.00, 4.46	1.00, 1.17
50	0.084 (0.314)	1.42 (0.46)	1.09 (0.04)
	−0.963, 1.0	1.00, 4.56	1.00, 1.21
100	0.092 (0.303)	1.59 (0.62)	1.12 (0.05)
	−1.0, 0.867	1.01, 8.09	1.01, 1.37
200	0.079 (0.29)	1.85 (1.56)	1.13 (0.05)
	−0.720, 1.0	1.03, 10.86*	1.03, 1.38
500	0.051 (0.256)	3.10 (7.82)	1.16 (0.06)
	−0.860, 1.0	1.04, 9.75*	1.01, 1.45
1000	0.044 (0.259)	5.02 (17.52)	1.17 (0.05)
	−0.777, 0.817	1.08, 10.59*	1.05, 1.37

For window-sizes greater than 100 m, the maximum sinuosity value has been adjusted by removing small islands having perimeters less than or very near the window-size (denoted with *)

The correlation coefficient did not significantly change with scale for absolute BCI versus fractal dimension. These results indicate that boundary convexity is a unique linear metric.

Coastal river otter latrine site selection

Model selection results indicate that BCI values at the 100 m window-size best approximated latrine presence (Table 2). Additionally, models of BCI at any of the window-sizes were found to be more parsimonious than any of the other metrics compared in the candidate set (Table 2). Because the global model was found to fit the data (no over-dispersion; Hosmer–Lemeshow GOF, $P > 0.05$), all candidate models will also fit the data.

To test the accuracy of the best-fitting models, models with the highest w_i for each patch boundary metric were assessed using leave-one-out cross-validation. Overall correct classification rate was highest for the model containing BCI at the 100 m scale (C100), with total prediction accuracy equaling 69.5% (Table 3). For each of the three additional models tested for accuracy, results demonstrate that total prediction accuracy is not much better than a coin-flip (Table 3). This observation is further supported by the relatively low AUC values for the three additional models, absolute convexity at 100 m, sinuosity at 500 m, and fractal dimension at 10 m (Fig. 6; Swets 1988).

Discussion

The value of a landscape metric is often specific to the landscape and species combination unique to a study area (Ritters et al. 1995). Li and Wu (2004) suggest that field or map based metrics will most often provide the greatest amount of inference because of their simplicity and ease of interpretation. Additionally, a landscape metric must be biologically meaningful and capture different aspects of spatial pattern (Ritters et al. 1995; Hargis et al. 1998; Li and Wu 2004). The boundary convexity index (BCI) meets these criteria for several reasons: (1) the metric is easily interpreted (positive or negative value); (2) the metric is scale-independent; (3) the metric captures different aspects of spatial pattern (i.e. not correlated with sinuosity or fractal dimension); (4) the metric is calculated at the 'sub-patch' scale; and (5) the metric was demonstrated to be biologically meaningful to coastal river otters (logistic regression analysis). Therefore, we feel that boundary convexity is an important new landscape metric that can be applied to any linear feature(s) of interest such as patch or landscape boundaries.

The shape of a boundary is specific to each unique location along that boundary and the shape is scale dependent. For example, a segment of coastline viewed using a 100 m frame may appear to be convex. However, the same location, when viewed at a scale of 1,000 m, may be concave in shape because the location may be within a larger bay. Thus, for any

Table 2 Summary of model selection statistics for the set of candidate models (*i*) predicting presence of otter latrines

Model	AIC_c	Δ AIC_c	w_i
C100	750.565	0	0.9993
C200	765.086	14.521	0.0007
C50	789.712	39.146	0
C500	802.806	52.241	0
C1000	816.431	65.865	0
C20	856.201	105.636	0
C10	866.632	116.067	0
AC100	891.434	140.869	0
S500	892.539	141.974	0
S1000	895.998	145.432	0
AC50	896.77	146.205	0
AC200	900.393	149.827	0
FD10	902.736	152.17	0
S200	906.24	155.675	0
S10	907.376	156.811	0
FD20	907.617	157.051	0
AC20	908.016	157.451	0
FD200	908.791	158.226	0
FD50	908.97	158.405	0
FD1000	909.001	158.436	0
AC10	909.086	158.521	0
AC1000	909.263	158.698	0
AC500	909.474	158.909	0
S100	909.716	159.15	0
FD100	909.841	159.275	0
FD500	909.853	159.287	0
S20	909.895	159.33	0
S50	909.901	159.336	0

Model descriptions are boundary convexity index (C), absolute boundary convexity index (AC), sinuosity (S) and fractal dimension (FD) followed by the window-size

Table 3 Percent of correctly classified observations using the best-fitting model for each patch boundary metric and leave-one-out cross-validation

Model	Latrine (%)	Random (%)	Total (%)
C100	69.6	69.3	69.5
AC100	51.5	66.0	58.7
S500	19.0	84.4	51.7
FD10	51.5	58.9	55.2

Model descriptions are boundary convexity index (C), absolute boundary convexity index (AC), sinuosity (S) and fractal dimension (FD) followed by the window-size

ecological problem, measuring variables at an appropriate scale (or range of scales) will require system and/or organism-specific knowledge (Allen and Hoekstra 1992). Measurements of boundary convexity performed to expectations when applied to a line with known dimensions. Boundary convexity values were consistently concave for troughs and convex for peaks and the values were identical in magnitude (with signs reversed) when measured from complementary locations on the regular artificial boundary. These measurements serve to characterize the boundary convexity metric and further, to demonstrate the range of values to expect under known conditions. However, we caution that comparing boundary convexity values between two datasets that have different 'reference scales' (i.e. 1:1,500 vs. 1:24,000) is not appropriate, even if the window-sizes are the same. This is true also for sinuosity and fractal dimension because the degree of generalization of line features from reality can differ greatly depending on the scale at which the data was digitized (acquired).

As mentioned above, the use of the coastline (a patch boundary) by coastal river otters within the study area is nearly ubiquitous, yet otter latrine site locations are found only where habitat conditions meet certain criteria (Bowyer et al. 2003). Using the shape (convexity) of the surrounding coastline as a variable influencing latrine site selection appears to be a promising landscape-scale metric. The logistic regression analysis supports our hypothesis that river otters may be selecting "points" as latrine sites, presumably to facilitate social communication via maximum dispersal of scent-marks. The measurement of boundary convexity for latrine sites at multiple scales allowed us to determine the scale at which otters most strongly respond to the shape of the coastline. This result improves our understanding of the scale at which river otters are interacting with their environment, and also will allow us to predict nutrient deposition by river otters in unsampled areas based in part on coastal shape. Using only a single variable (BCI at the 100 m scale), we were able to correctly classify nearly 70% of coastal locations as latrines. While previous attempts to determine habitat variables driving otter latrine site selection correctly classified 80–87% of locations, these studies measured habitat variables intensively at fine scales (Bowyer et al. 2003). The ability to

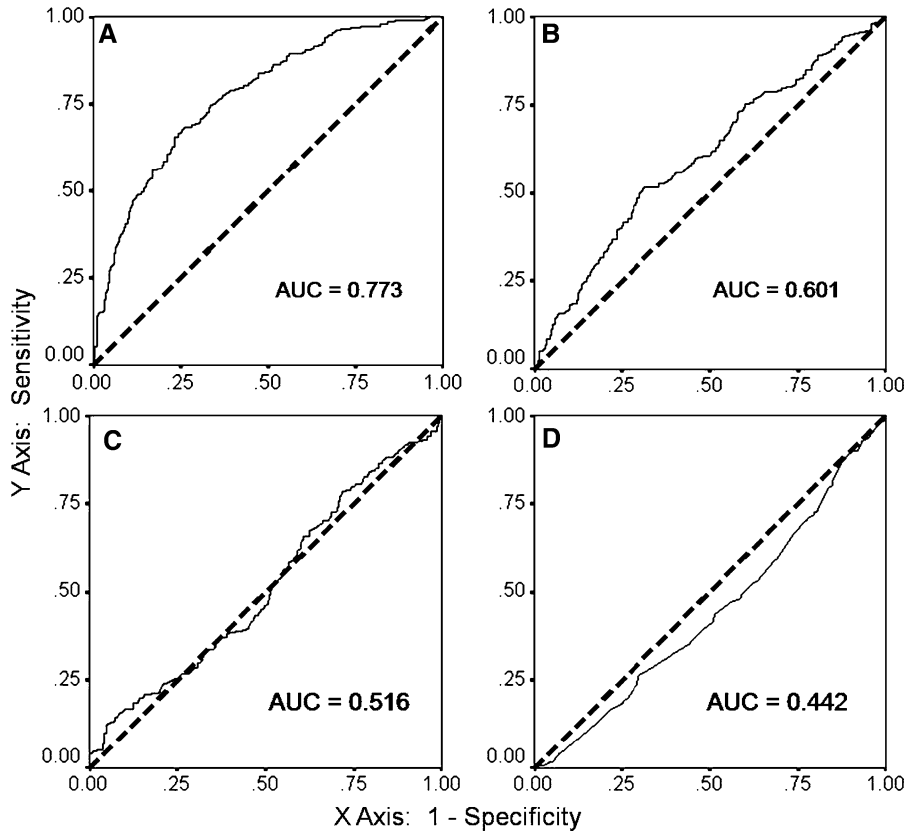

Fig. 6 ROC plots demonstrating discriminatory accuracy for otter latrine site selection for models: boundary convexity index at 100 m (**a**), absolute boundary convexity index at 100 m (**b**), sinuosity at 500 m (**c**) and fractal dimension at 10 m (**d**); and the calculated area under the curve (AUC)

predict otter latrine locations using data derived from satellite imagery will be invaluable for the management of coastal river otters and for understanding their role in nutrient transport from sea to land.

Boundary convexity could be applied to similar ecological questions where species depend on ecotones (unique conditions of patch boundaries). For example, Howell et al. (2007) found that brown-headed cowbird (*Molothrus ater*) use of forest edge varied by landscape context. Highly fragmented forests were used more completely than less fragmented forests. Would telemetry locations of female cowbirds demonstrate a relationship with boundary convexity? Taylor et al. (2008) found that the noisy miner (*Manorina melanocephala*) in Victoria, Australia were more likely to occur with edge geometry characteristics that were described as 'projections' and 'clumps'. Boundary convexity may provide a more quantitatively derived metric for describing the habitat use of this avian species. Other potential ecological situations in which boundary convexity could be applied are flying squirrel (*Pteromys volans*) dispersal which can be affected by landscape structure (Selonen and Hanski 2004) and arthropod densities that rely on algal wrack and carrion washed ashore on islands located in the Gulf of California (Polis and Hurd 1996).

In conclusion, boundary convexity measures spatial patterns at the sub-patch scale and can be used to help explain some ecological processes occurring along patch boundaries. Our research demonstrates how boundary convexity can be used to assess animal habitat selection based on this pattern. We hope the boundary convexity metric finds wide application, and further that the Boundary Convexity Tool (Albeke et al. 2009) will assist in the expanded use of not only boundary convexity, but also other linear metrics in a scalable, moving-window framework.

Acknowledgments We thank K. Ott, J. Herreman, B. Myers, K. Pope, T. Whitaker and M. Wood for valuable assistance in the field. Additional logistical support was provided by the Alaska Department of Fish and Game and Babkin Charters Inc. Additionally, we would like to thank the editors for their

insightful review of earlier versions of this manuscript. Funding for this project was provided by the University of Georgia, Warnell School of Forestry and Natural Resources and a grant from the National Science Foundation (NSF #0454474) to M. Ben-David, N. Nibbelink, and C. Meyer.

References

Albeke SE, Nibbelink NP, Mu L, Ellsworth DJ (2009) Boundary convexity tool. University of Georgia, Athens. http://arcscripts.esri.com/details.asp?dbid=16165. Accessed 14 Apr 2009

Allen TFH, Hoekstra TW (1992) Toward a unified ecology. Columbia University Press, New York, NY

Anderson DR, Burnham KP, Thompson WL (2000) Null hypothesis testing: problems, prevalence, and an alternative. J Wildl Manag 64:912–923

Ben-David M, Bowyer RT, Duffy LK, Roby DD, Schell DM (1998) Social behavior and ecosystem processes: river otter latrines and nutrient dynamics of terrestrial vegetation. Ecology 79:2567–2571

Ben-David M, Blundell GM, Kern JW, Maier JAK, Brown ED, Jewett SC (2005) Communication in coastal river otters: creation of variable resource sheds for terrestrial communities. Ecology 86:1331–1345

Bowyer RT, Blundell GM, Ben-David M, Jewett SC, Dean TA (2003) Effects of the Exxon Valdez oil spill on river otters: injury and recovery of a sentinel species. Wildl Monogr 153:1–53

Burnham KP, Anderson DR (2001) Kullback–Leibler information as a basis for strong inference in ecological studies. Wildl Res 28:111–119

ESRI (2006) ArcGIS: Release 9.2 [software]. Environmental Systems Research Institute, Redlands, CA

Ewers RM, Didham RK (2007) The effect of fragment shape and species' sensitivity to habitat edge on animal population size. Conserv Biol 21:926–936

Forester JD, Ives AR, Turner MG, Anderson DP, Fortin D, Beyer HL, Smith DW, Boyce MS (2007) State-space models link elk movement patterns to landscape characteristics in Yellowstone National Park. Ecol Monogr 77: 285–299

Grober-Dunsmore R, Frazer TK, Beets JP, Lindberg WJ, Zwick P, Funicelli NA (2008) Influence of landscape structure, on reef fish assemblages. Landscape Ecol 23: 37–53

Hamer TL, Flather CH, Noon BR (2006) Factors associated with grassland bird species richness: the relative roles of grassland area, landscape structure, and prey. Landscape Ecol 21:569–583

Hargis CD, Bissonette JA, David JL (1998) The behavior of landscape metrics commonly used in the study of habitat fragmentation. Landscape Ecol 13:167–186

Haynes KJ, Cronin JT (2006) Interpatch movement and edge effects: the role of behavioral responses to the landscape matrix. Oikos 113:43–54

Heegaard E, Okland RH, Bratli H, Dramstad WE, Engan G, Pedersen O, Solstad H (2007) Regularity of species richness relationships to patch size and shape. Ecography 30:589–597

Hopkins RL (2009) Use of landscape pattern metrics and multiscale data in aquatic species distribution models: a case study of a freshwater mussel. Landscape Ecol 24: 943–955

Hosmer DW, Lemeshow S (2000) Applied logistic regression. Wiley, New York

Howell CA, Dijak WD, Thompson FR III (2007) Landscape context and selection for forest edge by breeding brown-headed cowbirds. Landscape Ecol 22:273–284

Kearns FR, Kelly NM, Carter JL, Resh VH (2005) A method for the use of landscape metrics in freshwater research and management. Landscape Ecol 20:113–125

Kie JG, Ager AA, Bowyer RT (2005) Landscape-level movements of North American elk (*Cervus elaphus*): effects of habitat patch structure and topography. Landscape Ecol 20:289–300

King G, Tanner MA, Rosen O (2004) Ecological inference: new methodological strategies. Cambridge University Press, Cambridge, UK

Larsen DN (1983) Habitats, movements, and foods of river otters in coastal southeastern Alaska, University of Alaska, Fairbanks, Alaska, 169 pp

Li BL (2000) Fractal geometry applications in description and analysis of patch patterns and patch dynamics. Ecol Model 132:33–50

Li H, Wu J (2004) Use and misuse of landscape indices. Landscape Ecol 19:389–399

Mandelbrot BB (1982) The fractal geometry of nature. W. H. Freeman, San Francisco

McGarigal K, Cushman SA, Neel MC, Ene E (2002) FRAGSTATS: spatial pattern analysis program for categorical maps. University of Massachusetts, Amherst. http://www.umass.edu/landeco/research/fragstats/fragstats.html. Accessed Jan 2007

McGrath MT, DeStefano S, Riggs RA, Irwin LL, Roloff GJ (2003) Spatially explicit influences on northern goshawk nesting habitat in the interior Pacific northwest. Wildl Monogr 154:1–63

Mitchell MS, Lancia RA, Gerwin JA (2001) Using landscape-level data to predict the distribution of birds on a managed forest: effects of scale. Ecol Appl 11:1692–1708

Nams VO, Mowat G, Panian MA (2006) Determining the spatial scale for conservation purposes—an example with grizzly bears. Biol Conserv 128:109–119

Polis GA, Hurd SD (1996) Linking marine and terrestrial food webs: allochthonous input from the ocean supports high secondary productivity on small islands and coastal land communities. Am Nat 147:396–423

Rempel R (2008) Patch analyst 4. Centre for Northern Forest Ecosystem Research (Ontario Ministry of Natural Resources), Lakehead University. http://flash.lakeheadu.ca/~rrempel/patch/index.html. Accessed Jan 2008

Ritters KH, O'Neill RV, Hunsaker CT, Wickham JD, Yankee DH, Timmins SP, Jones KB, Jackson BL (1995) A factor analysis of landscape pattern and structure metrics. Landscape Ecol 10:23–39

Robinson WS (1950) Ecological correlations and the behavior of individuals. Am Sociol Rev 15:351–357

Roe AM, Meyer CB, Nibbelink NP, Ben-David M (2010) Differential production of trees and shrubs in response to fertilization and disturbance by coastal river otters in Alaska. Ecology. doi:10.1890/09-1216.1

Rostain RR, Ben-David M, Groves P, Randall JA (2004) Why do river otters scent-mark? An experimental test of several hypotheses. Anim Behav 68:703–711

Ruiz D, Escribano C, Fernandez-Quintanilla C (2006) Identifying associations among sterile oat (*Avena sterilis*) infestation level, landscape characteristics, and crop yields. Weed Sci 54:1113–1121

Selonen V, Hanski IK (2004) Young flying squirrels (*Pteromys volans*) dispersing in fragmented forests. Behav Ecol 15: 564–571

Steyerberg EW, Frank E, Harrell J, Borsboom GJJM, Eijkemans MJC, Vergouwe Y, Habbema JDF (2001) Internal validation of predictive models: efficiency of some procedures for logistic regression analysis. J Clin Epidemiol 54:774–781

Swets JA (1988) Measuring the accuracy of diagnostic systems. Science 240:1285–1293

Taylor RS, Oldland JM, Clarke MF (2008) Edge geometry influences patch-level habitat use by an edge specialist in south-eastern Australia. Landscape Ecol 23:377–389

Trani MK, Giles RH (1999) An analysis of deforestation: metrics used to describe pattern change. For Ecol Manag 114:459–470

Turchin P (1996) Fractal analyses of animal movement: a critique. Ecology 77:2086–2090

Turner MG (1989) Landscape ecology—the effect of pattern on process. Annu Rev Ecol Syst 20:171–197

Wu J (2004) Effects of changing scale on landscape pattern analysis: scaling relations. Landscape Ecol 19:125–138